

BEAM LOSS STUDY OF TLS USING RadFETs

C. H. Huang, S.H. Lee, Y.S. Cheng, K. H. Hu, C. Y. Wu, J. Chen, K. T. Hsu
 NSRRC, Hsinchu 30076, Taiwan

Abstract

To realize the beam loss during the operation of Taiwan light source, P-type radiation-sensing field-effect transistors are setup around the storage ring. A sixteen-channel readout box is used to read the threshold voltage of the radiation-sensing field-effect transistors during irradiation. The beam loss distribution and mechanism at the injection period, decay mode and top up injection for routing operation will be studied in this report.

INTRODUCTION

The radiation-sensing field-effect transistor (RadFET) is a discrete p-channel metal-oxide-semiconductor field-effect transistor optimized for ionizing radiation [1]. Through detecting the voltage between the gate and source caused by the radiation-induced charges in the gate oxide during a forcing current, the radiation dose is obtained by a pre-recorded calibration curve.

For the last two decades, RadFETs have been found wide applications in the particle accelerator environment [2], space and clinical control. For a synchrotron light source such as Taiwan light source (TLS), the RadFET will be a useful device to detect beam loss due to the Touschek effect, the residual gas scattering, the intra-beam scattering and so on [3].

TLS is a synchrotron light source which equips with six-fold symmetry and three-bend achromatic (TBA) cells in storage ring. Its circumference is 120 m and the operating energy is 1.5 GeV. It equips with insertion devices including U50, U90, EPU56, W200, superconducting wavelength shifter (SWLS) and superconducting wiggler (SW60) in six 6-m long straight sections. Three identical superconducting wigglers (IASWR2, IASWR4, IASWR6) are installed in achromatic cells between the first and the second bending magnets of the second, fourth and sixth TBA cells.

RADFET READER SYSTEM

In order to achieve high density installation of the RadFETs, the reader is designed to link up to sixteen RadFETs with RJ-45 connectors and unshielded-twisted-pair network cables, as shown in Fig. 1. In the radiation exposure period, the gate voltage is zero-biased now or +5V for the positive-biased applications. In the readout period, a DC current with 12.5 μ A is forcing into the gate for several seconds to obtain the threshold voltage (V_{th}) in the reader circuit configuration. The readout period is one minute now and the threshold voltage is readout one by one through a 24-bit analog-to-digital convertor (ADC). The control processes are programmed in the input / output controller (IOC) of the experimental physics and

industrial control system (EPICS) and process variables (PVs) are published into the control network. An operation interface is designed to show the threshold voltage of RadFETs, accumulated dose, dose rate and dose rate distribution. The threshold voltage of RadFETs are recorded in the archive server for further analysis after the experiment [4].

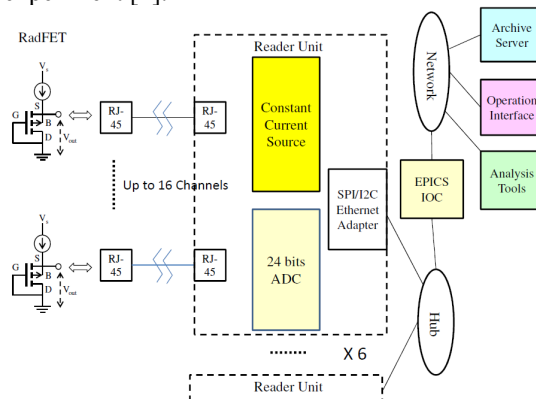


Figure 1: Block diagram of the RadFET readers' setup.

EXPERIMENTAL SETUP AND RESULTS

Six readers are setup below the girder of the second bending magnet in each cell of the storage ring to minimize the possible radiation damage, shown in Fig. 2(a). The uplink cables of six readers are connected to an Ethernet switch to form as a private network and then connect to the IOC in the equipment area of the TLS. In the first step, the two RadFETs are setup in the blue square position of Fig. 3 with one in the inside wall of the vacuum chamber shown in Fig. 2(b) and the other in the outside wall of the chamber in the storage ring.

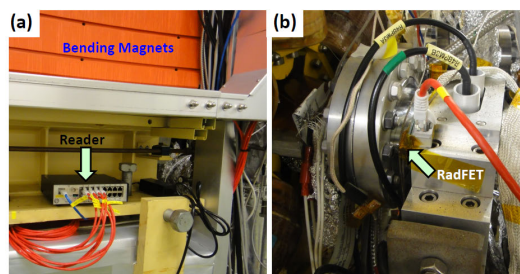


Figure 2: The setup of the (a) reader and (b) RadFET.

As the machine operates on the top-up mode, the detected radiation in the inside wall of the chamber is mostly larger than that in the outside wall, shown in Fig 4. That is because the beam loss caused by Touschek effect contributes into both sides but the beam loss caused by Bremsstrahlung only contributes to the inside wall. The detected dose rate is smaller than 0.3 Gy/hr except the

RadFET #1 which is installed between the injection area and the 1st bending magnet of the 1st cell. The RadFETs in the position #1, where the vertical beta function is large, detect more radiation in the outside-wall RadFETs than that inside-wall RadFETs. The beam loss in this area may be owing to the small gap in the injection area.

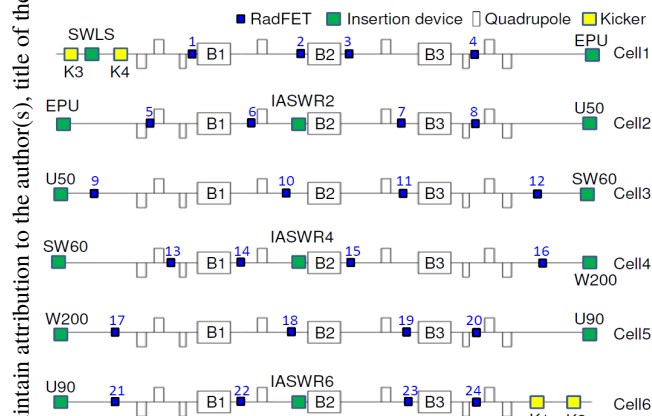


Figure 3: The setup position of the RadFETs in the storage ring with one in the inside wall of the chamber and the other in the outside wall of the chamber.

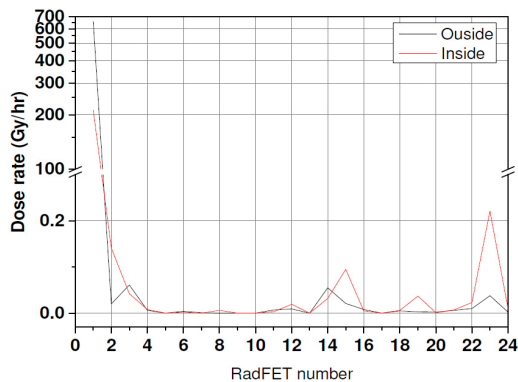


Figure 4: The beam loss distribution in the top-up mode for the beam current is between 361-362 mA.

To realize the beam loss around the injection area, the comparison between the beam current and radiation dose rate is shown in Fig. 5. It is clear that the detected dose rate is almost proportional to the beam current no matter in the injection, top-up, decay or dump beam period. The dose rate arising after injecting may be because of the interface states build-up after irradiation [5].

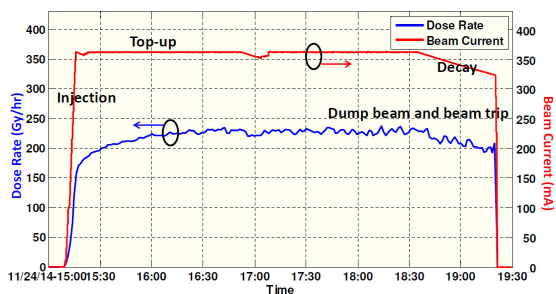


Figure 5: The comparison between the beam current and the dose rate of radiation detected by the RadFET installed in inside-wall chamber of position #1.

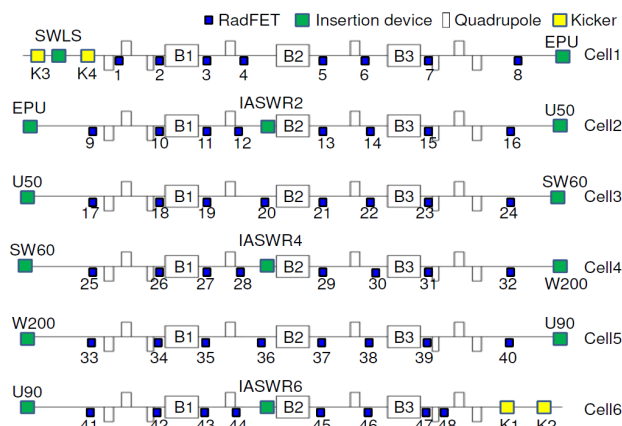


Figure 6: The setup position the RadFETs in the inside wall of the chamber.

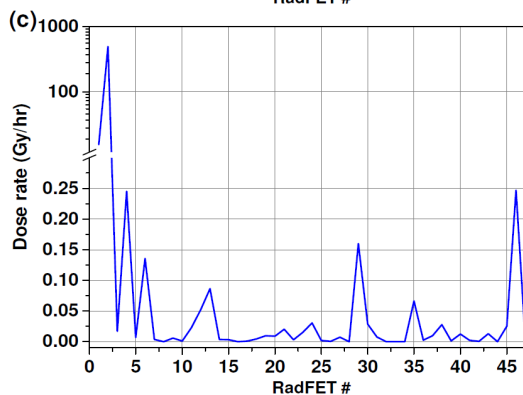
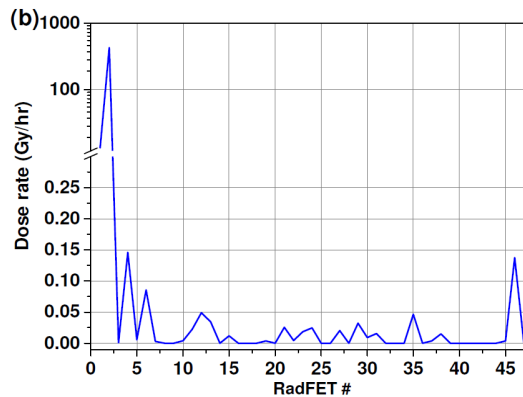
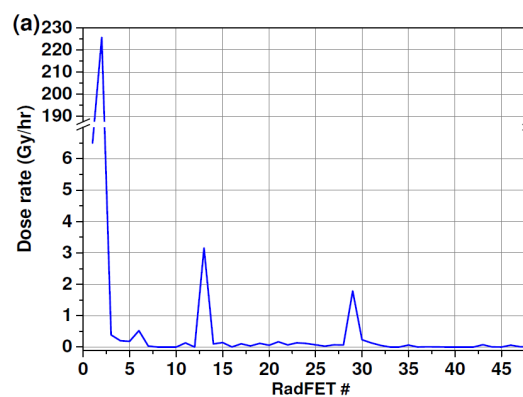


Figure 7: Beam loss distribution (a) as injecting from 0 to 362 mA, (b) as decaying from 360 to 307 mA and (c) in top-up injection between 361 and 362 mA.

In the second step, the RadFETs are all moved to the inside wall of the chamber, shown in Fig. 6. Similarly as the setup in the first step, the most radiation is detected by the RadFET which is installed before the 1st bending magnet (B1) of the 1st cell, shown in Fig. 7. In the injection period from 0 to 362 mA, the beam loss in Fig. 7 (a) mainly happens at the 2nd bending magnet of 2nd cell and 4th cell besides the injection area. It should be that some electrons hit chamber within IASWR2 and IASWR4 due to the small gap and lose the energy. The energy-lost beam will get lost after the following bending magnets. In the decay mode, the beam loss in Fig. 7 (b) is smaller than that in the injection period and top-up mode. For the top-up injection in Fig. 7 (c), the main loss happened at injection area and after the bending in the 2nd, 4th and 6th cell. The mechanism should be the same with that in the injection period.

At beam trip event caused by the radio frequency (RF) system in the machine study shift, beam is largely lost after the 1st bending magnet of the 1st cell, shown in Fig. 8. As we know, the dispersion is largest after the 1st bending magnet and before the 3rd bending magnet for the TBA lattice. The beam trajectory will bend toward the inside wall of the chamber significantly at high dispersion region as energy is lower than the nominal one. The small gap in the injection read and high dispersion may make the most beams lose at this region.

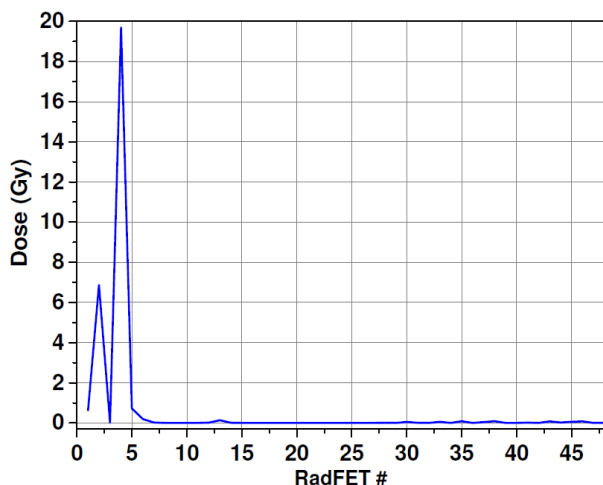


Figure 8: The accumulated dose during the beam trip caused by the RF system.

THE APPLICATION IN THE TAIWAN PHOTON SOURCE

This data acquisition system is also used to study the beam loss in the linac to booster (LTB) [6] and booster ring during beam commissioning of Taiwan photon source (TPS). For the booster ring, the RadFETs are installed before the fifty-four bending magnets in six cells. Nine RadFETs in one cell are collected by a reader. Six readers and the controlling IOC is linked with a private virtual LAN. The accumulated dose, dose rate and beam loss distribution are published and shown in the control system online. Figure 9 shows the beam loss distribution

during TPS commissioning. In the future, that would be setup in the storage ring of TPS to study the beam loss mechanism.

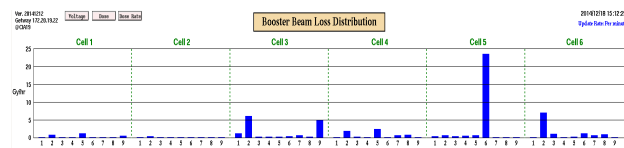


Figure 9: Beam loss distribution of booster ring during beam commissioning of Taiwan photon source.

CONCLUSION

RadFETs are used to study the beam loss of TLS. The beam loses significantly in the downstream of the injection area. The radiation loss detected by the RadFET before the 1st bending magnet in the 1st cell is much larger than the others no matter in the injection period, decay mode and top-up mode operation. The beam loss may be due to its small gap in this area.

Besides the injection area, beam loss can also be observed after the bending magnet following the IASWR2, IASWR4 and IASWR6. For the injection period, beam loses more serious after IASWR2 and IASWR4 but beam loss more seriously after IASWR6 in the decay mode. Therefore, beam loss can all be observed after IASWR2, IASWR4 and IASWR6 in the top-up mode. In the beam trip period caused by the RF system, beam loss is largest after the 1st bending in the 1st cell where the dispersion is largest. The beam trajectory will bend significantly toward the inner chamber in this area when the beam energy is less than the nominal one which would make the beam loss be observed here.

This system is also migrated into study the beam loss during the beam commissioning in TPS. The infrastructure is similar with that in TLS. In the future, it will be setup in the storing ring of TPS to realize the beam loss mechanism.

REFERENCES

- [1]. Jaksic, et al., "Characterisation of Radiation Response of 400nm Implanted Gate Oxide RadFETs", MIEL, Nish, Yugoslavia (2002).
- [2]. L. Frohich, et. al., Nucl. Instr. And Meth. A 703, p 77-79 (2013).
- [3]. O. A. Konstantinova, et al., "Beam Loss Studies for the KEK Compact-ERL", IPAC, Dresden, Germany (2014).
- [4]. Demi Lee, et al., "Online RadFET Reader for Beam Loss Monitoring System", these proceedings, IPAC, Richmond, USA (2015).
- [5]. D. M. Fleetwood, et al., J. Appl. Phys. 73 p 5058-5074 (1993).
- [6]. H. Huang, et al., "Diagnostics of the TPS Booster Synchrotron for Beam Commissioning", IBIC 2014, Monterey, USA.